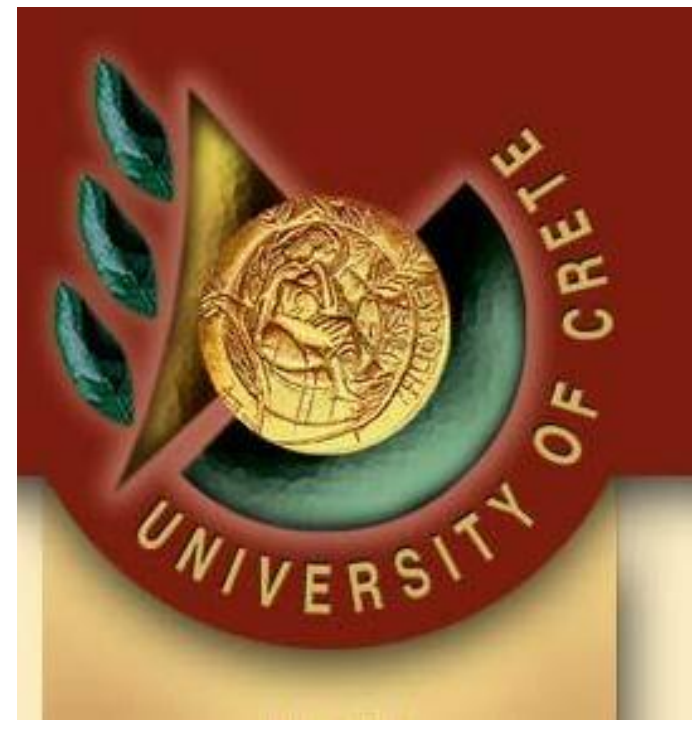




IMPROVING THE RESOLUTION OF A HEMISPHERICAL DEFLECTOR ANALYZER (HDA): DESIGN AND PERFORMANCE OF A BIASED PARACENTRIC HDA



Theo J. M. Zouros^{1,2} (tzouros@physics.uoc.gr), Omer Sise³, Melike Ulu³, Mevlut Dogan³

¹Department of Physics, University of Crete, P.O. Box 2208, 71003 Heraklion, Crete, and

²Tandem Accelerator Laboratory, NCSR "Demokritos", 15310 Aghia Paraskevi, Athens, GREECE

³Department of Physics, Science and Arts Faculty, Afyon Kocatepe University, 03200 Afyonkarahisar, TURKEY

Abstract

The first-order focusing characteristics of deflection type energy mirror analyzers are impaired due to fringing fields at the electrode boundaries. In the conventional hemispherical deflector analyzer (HDA), fringing fields generally create an image with angular aberrations at the dispersion plane. This drawback is, to a large extent, overcome has been shown in simulation, for the "biased paracentric" HDA which has a biased optical axis and an optimized entry position offset (paracentric) from the center position used in conventional HDAs. Using a special experimental setup, we present here first measurements which clearly demonstrate the improved resolution in good overall agreement with simulation.

MOTIVATION

Hemispherical deflector analyzers (HDAs) combined with a cylindrical input-lens-system are widely used to analyze the energy of charged particle beams, providing fairly high transmission and energy resolution. In particular, the elimination of aberrations caused by the inherent fringing fields at the boundaries of electrodes is of primary concern (See Fig. 1). Fringing fields distort the ideal field trajectories, and hence change the energy dispersion across the exit plane, as well as changing the aberration properties of the HDA. Correction schemes usually involve the addition of biased electrodes. However, for the biased paracentric entry HDA [1-3], no additional electrodes are needed (see Fig. 6).

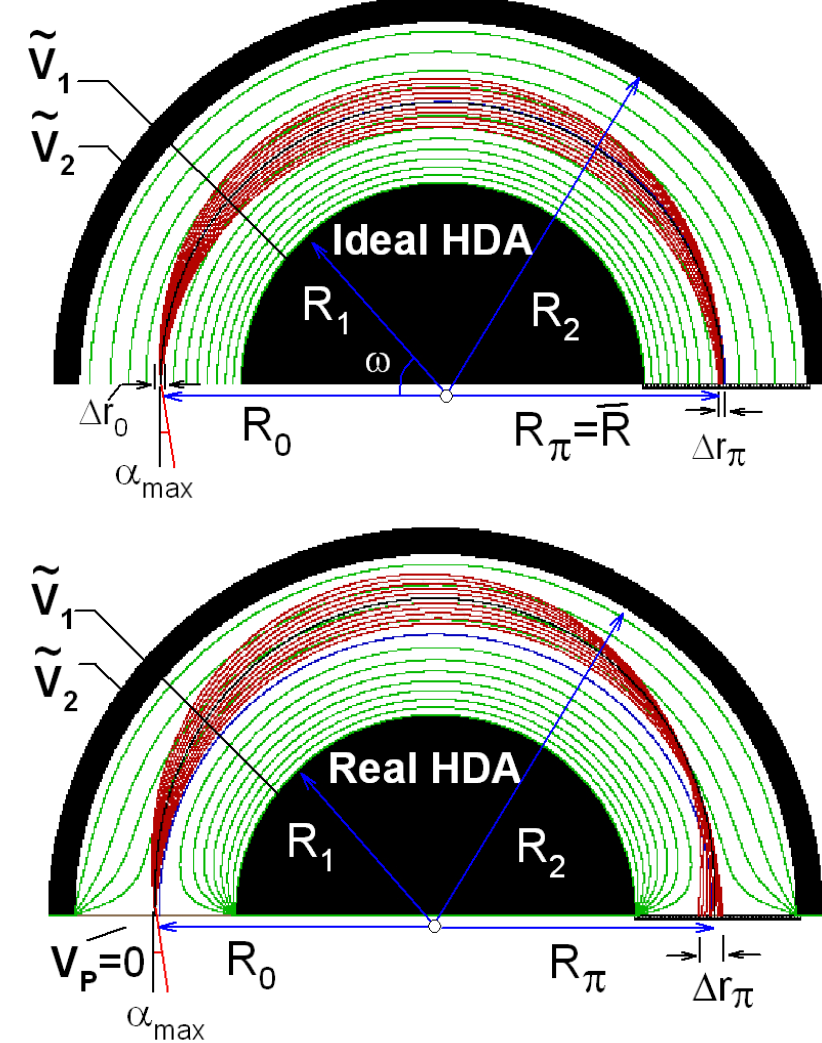


Figure 1: Electron trajectories for 10 different launching angles for both ideal and fringing field conventional HDA. At the entry, the beam is taken to be a point-like source.

INSTRUMENT

The components of the biased paracentric HDA constructed in this work are shown in Fig. 2. The analyzer system consists of a hemispherical deflector, a movable five-element input lens, and a single channel electron multiplier. The hemispherical deflector consists of concentric hemispherical outer and inner electrodes with radii $R_1=75\text{ mm}$ and $R_2=125\text{ mm}$. The mean radius of the analyzer is 100 mm.



Figure 2: Components of the newly designed biased paracentric analyzer: (1) outer hemisphere, (2) inner hemisphere, (3) mounting (or deceleration) plate, (4) five-cylinder input lens, (5) grounded shield, (6) rail, (7) mounting part of the input lens, and (8) detector housing.

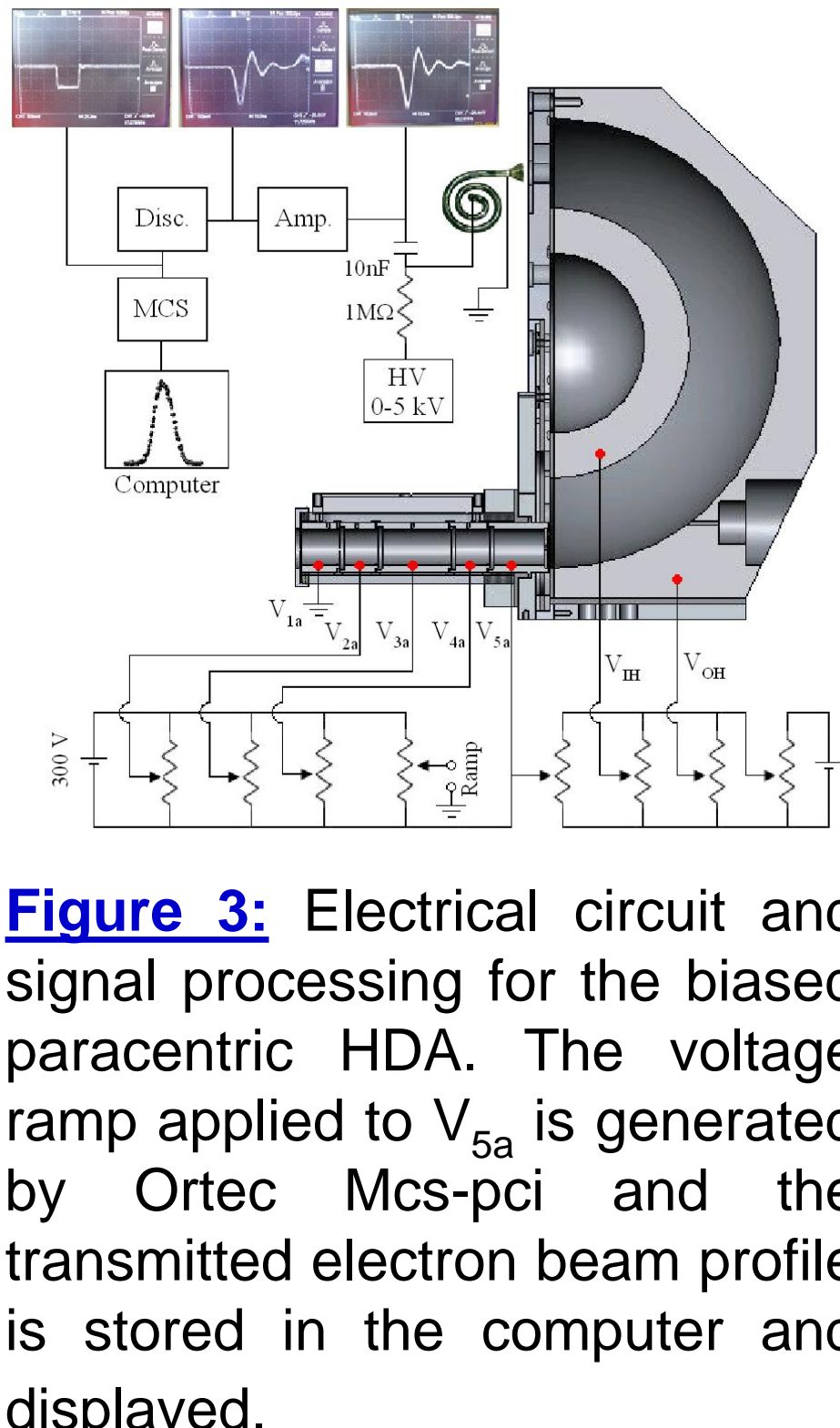


Figure 3: Electrical circuit and signal processing for the biased paracentric HDA. The voltage ramp applied to V_{5a} is generated by Ortec Mcs-pci and the transmitted electron beam profile is stored in the computer and displayed.

ACKNOWLEDGEMENTS

Partial support from the Turkish State Planning organization grant 2002K120110, TUBITAK grant 106T722, the Greek government and EU.

REFERENCES

- [1] Benis, Zouros, Nucl. Instr. Meth. Phys. Res. A **440**, L462 (2000); *ibid.* J. Elect. Spec. **125**, 221 (2002); *ibid.* **163**, 28 (2008)
- [2] Zouros, Sise, Ulu, Dogan, Meas. Sci. Tech. **17**, N81 (2006).
- [3] Sise, Zouros, Ulu, Dogan, Meas. Sci. Tech. **18**, 1853 (2007).

EXPERIMENTAL PROCEDURE

Based on electron optic simulations, a compact biased paracentric hemispherical deflector analyzer for atomic collisions has been designed and constructed (see Fig. 4). The performance of this analyzer has been tested by observing the elastic scattering of electrons on helium. Two different paracentric positions were studied and compared with the central position. For the paracentric entries, correction of the fringing field aberration is performed by additional biasing of the optical axis inside the analyzer by appropriately changing both electrode voltages.

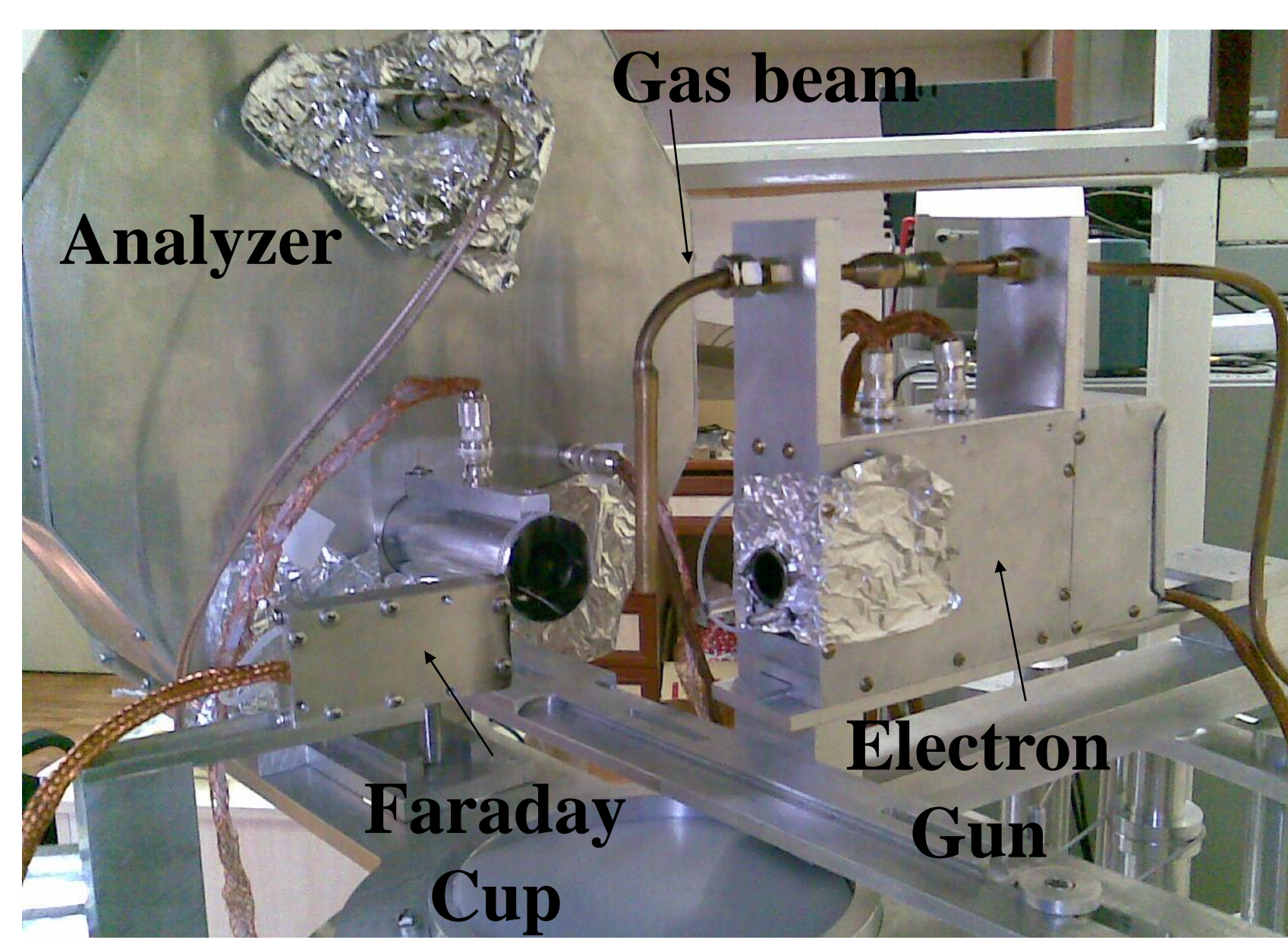


Figure 4: Photograph of the analyzer assembled on the shaft.

To obtain energy distributions at fixed resolution, the pass KE is fixed and the analyzer retarding voltage V_{5a} is varied to scan the desired energy range. The analyzer transmission function was studied by varying the bias while keeping the exit radius constant and measuring the total counts detected as the retarding voltage was ramped across the peak. The ramp voltage sequence is repeated until a pre-determined statistical accuracy is obtained.

RESULTS

In all of the experiments described here the energy of the electrons in the electron gun was set at 200 eV. Experiments were then carried out to obtain the peak structure of electrons at three entry positions, $R_0=84, 100$, and 112 mm , respectively, for four pass energies, $KE=30, 40, 50$, and 60 eV . The values of 84 and 112 mm were determined according to the scaling prescription described in Ref. [3].

The results from these measurements are shown in Figs. 5-7. The different spectra correspond to different bias values on the analyzer electrodes. To extract a peak position and full width at half maximum, a Gaussian distribution was fitted to the data. To demonstrate the focusing properties of the HDA, simulations of two-dimensional X-Y images were performed using 10⁵ electrons emitted from the source region. Their velocity vectors were uniformly distributed over a cone angle of $\alpha=3^{\circ}$. The bottom of Figs. 5-7 illustrate a sample set of electron trajectories that are emitted from the source and successfully reach the detector.

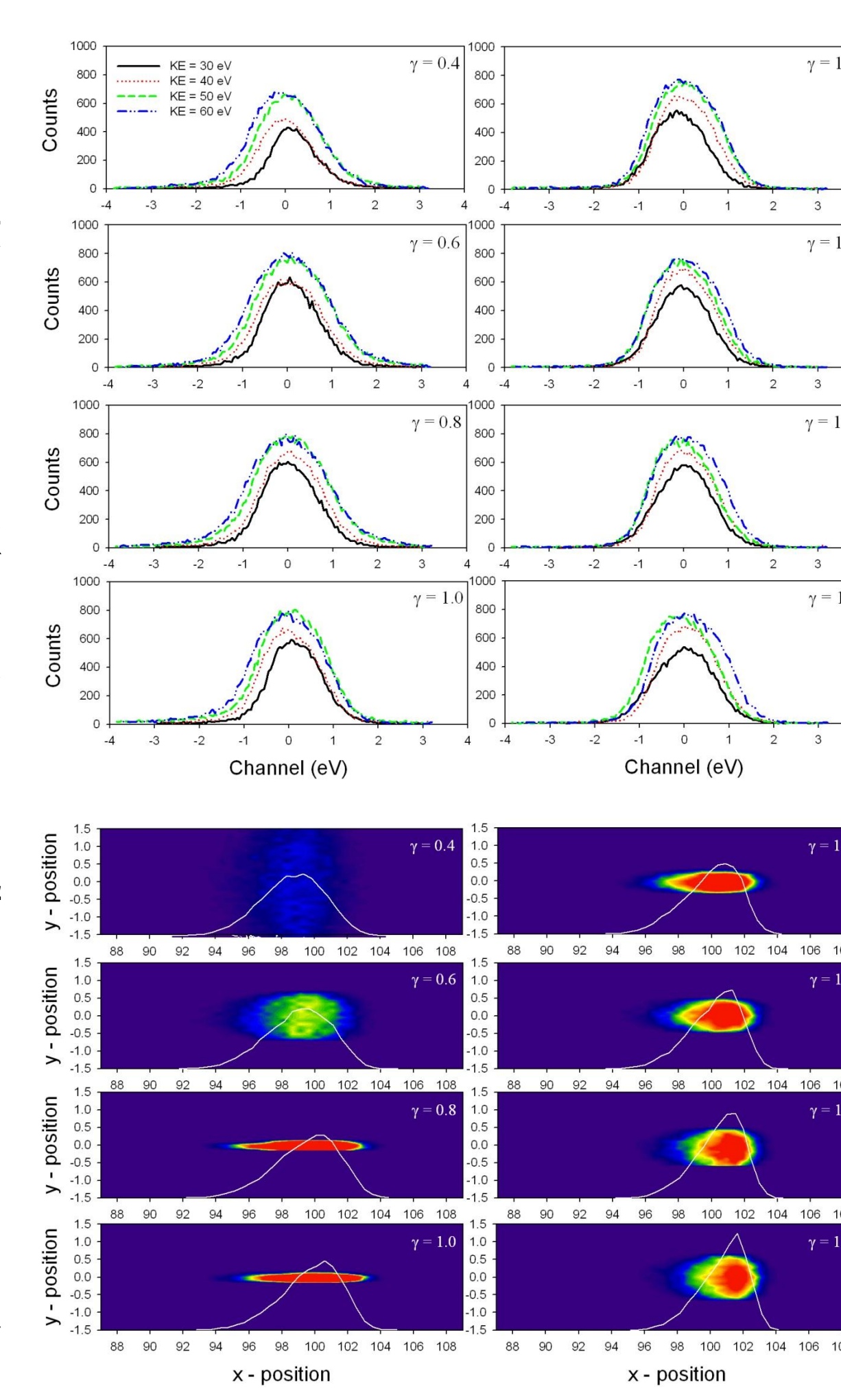


Figure 5. (Top) Electron kinetic energy spectrum showing the elastic scattering peak from 200 eV electrons incident on He for $R_0=100\text{ mm}$. The instrument was set to pass the $KE=30, 40, 50$, and 60 eV electrons, respectively. (Bottom) Two dimensional simulated X-Y images of the electrons on the detector obtained with $E_0=200\text{ eV}$, $E_{\text{pass}}=KE=50\text{ eV}$ and $\alpha=3^{\circ}$ for an extended source of $\Delta r=2\text{ mm}$. The projection along the dispersion direction is also plotted.

BIASED PARACENTRIC HDAs

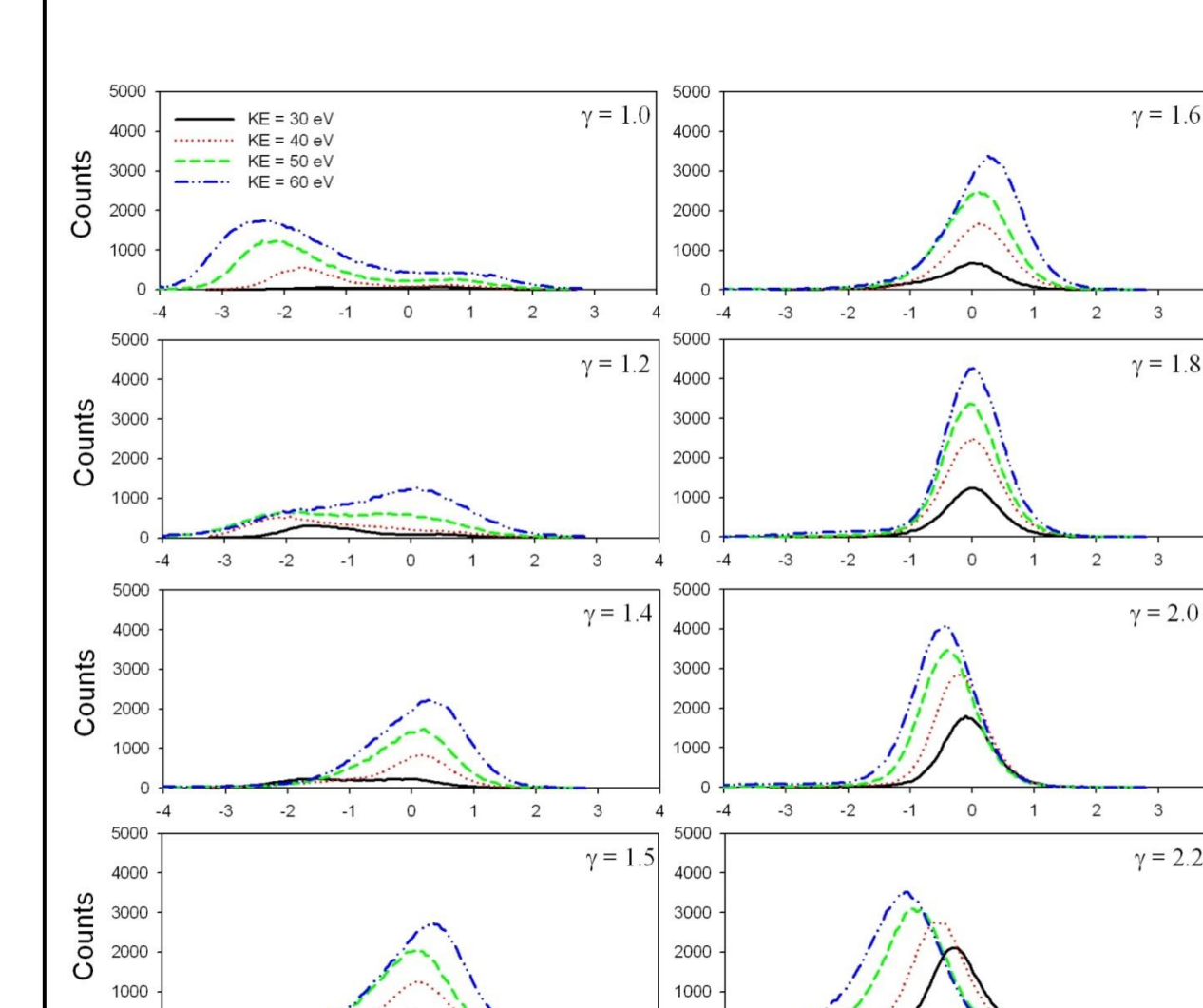


Figure 6. Same as Fig. 5, but for $R_0=84\text{ mm}$.

Unbiased entry ($\gamma=1$) is seen to result in a rather diffuse image at the PSD with a corresponding degradation of the energy resolution. A biased paracentric entry with $\gamma \sim 1.6$, however, is seen to give the best energy resolution.

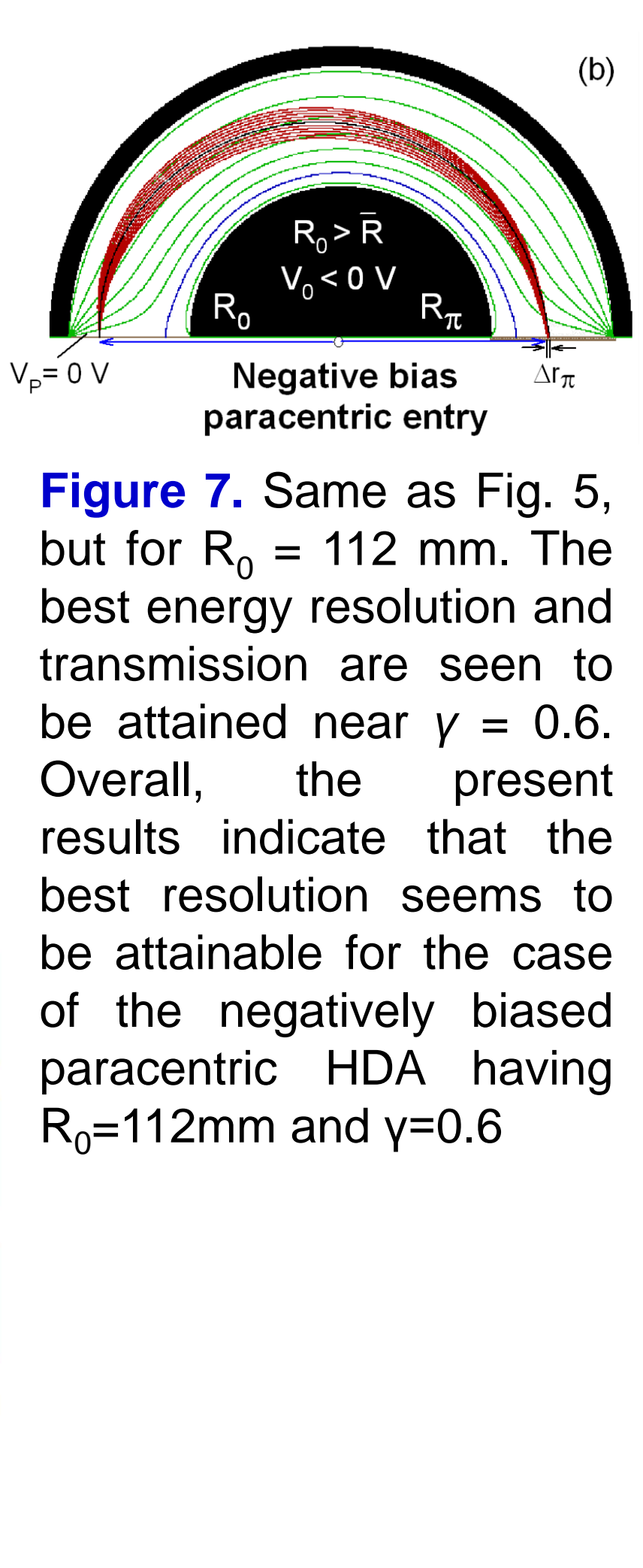


Figure 7. Same as Fig. 5, but for $R_0=112\text{ mm}$. The best energy resolution and transmission are seen to be attained near $\gamma=0.6$. Overall, the present results indicate that the best resolution seems to be attainable for the case of the negatively biased paracentric HDA having $R_0=112\text{ mm}$ and $\gamma=0.6$.

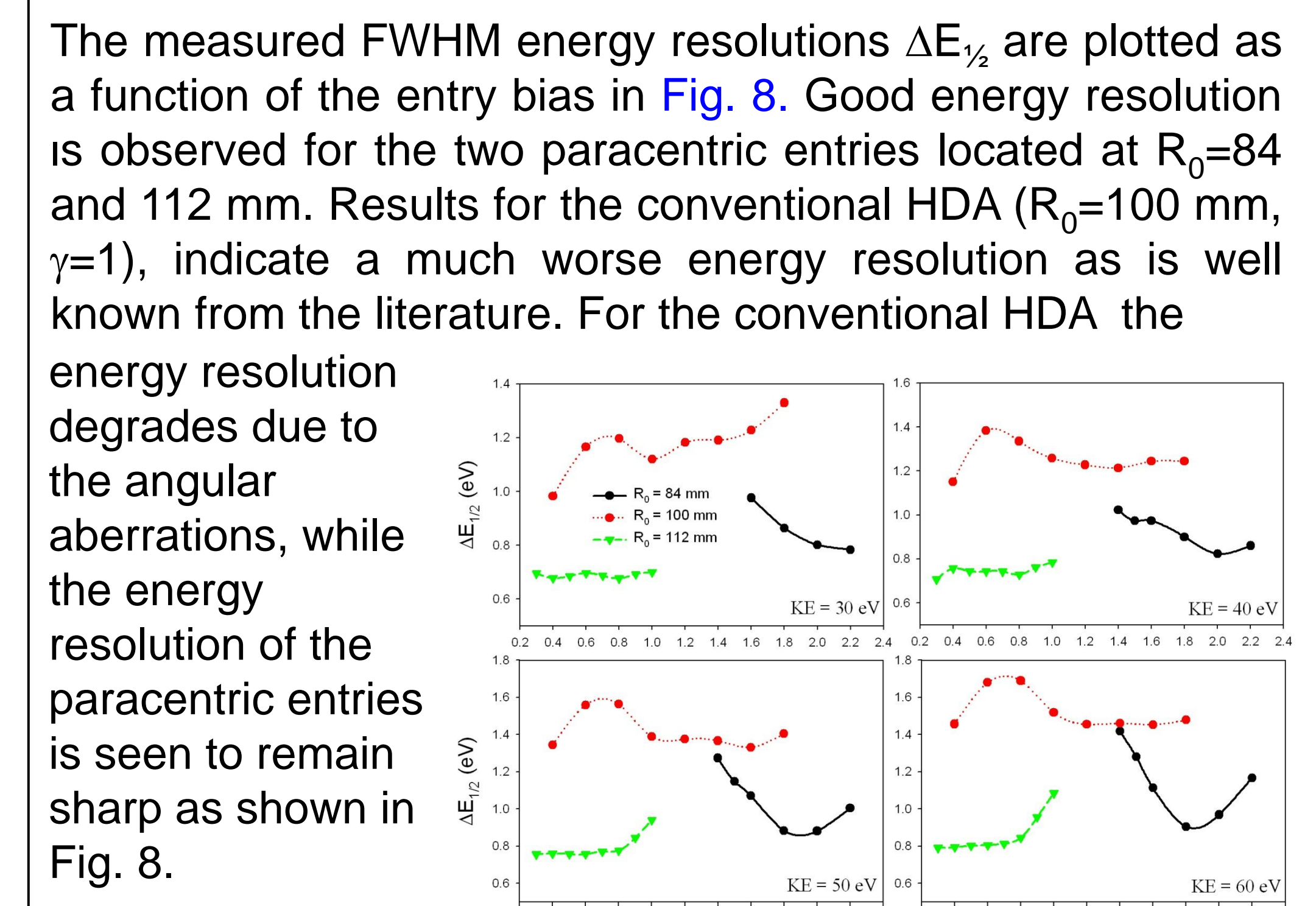


Figure 8. Experimental energy resolution for $R_0=84, 100$ and 112 mm under identical conditions. Resolution improvement of up to a factor of 2 relative to the $\gamma=1$ $R_0=100\text{ mm}$ centric HDA can be observed. Lines are used to guide the eye.

SUMMARY AND CONCLUSIONS

We have designed and constructed a biased paracentric HDA for measuring electron energies at three different entry positions. Our results demonstrate that the biased paracentric configurations show a much improved energy resolution and transmission compared to the conventional entry position *without* the need to use any type of additional fringing field corrector electrodes. Such an analyzer can be expected to provide high energy resolution combined with large sensitivity and simple design and should be particularly useful in HDAs using position sensitive detectors in low count rate experiments at XFEL and synchrotron facilities around the world.